CONTRIBUTIONS TO MINERALOGY AND RADIOACTIVITY OF WADI ABU MAYAH STREAM SEDIMENTS, CENTRAL EASTERN DESERT, EGYPT

EL AZAB

ABSTRACT

The area is far from the Red Sea about 40 km west of Safaga City. The wadi Abu Mayah is located south Qena-Safaga road. This wadi has long 30km, and width 50m to 200m, and covered by stream sediments. The rocks cropping out in the sides of wadi area are metagabbros (oldest), older granitoids, and younger granites (youngest).

The heavy content ranging from 2.9% and 9.4% and the average content of total heavy minerals is 5.4%. Opaque minerals represented by Magnetite, Ilmenite constituents have an average 1.2 %, and 0.4 % respectively. Abrasive minerals as Garnet constituents has an average 0.15%, and panting minerals as Rutile and Titanite constituents have an average 0.34%, and 0.15% respectively. Radioactive minerals as Zircon, Monazite, Apatite and Thorite constituents have an average 0.26%, 0.02%, 0.01, and 0.02 % respectively. Amphiboles and Pyroxene constituents range from 2.1% to 4.4% with an average 2.8 %. The eU contents range between 12 and 40ppm with an average 21.3ppm, while eTh is between 20 and 86ppm for with an average 38.2ppm. The average Ra content for these sediments is 2.9ppm, and the average content of K% is 1.5%.

INTRODUCTION

The Egyptian Eastern Desert, northern Sudan, western Saudi Arabia and Yemen have collectively been termed the Arabian Nubian Shield, which is characterized by four principal rock association: i.e. (1) an older shelf sequence of ortho- and paragnesis, (2) arc assemblages, (3) ophiolitic suits and (4) granitoid intrusive. The Egyptian granitoid rocks have been subdivided in different ways (Greenberg, 1981). They can be in general classified into two main types, the older and younger granites (El-Ramly and Akaad, 1960, Abdel-Rahman, 1990 and Akaad, et al., 1973. Abdel-Rahman, et al., 2006, studyied the significance of gneissic rocks and synmagmatic extensional ductile shear zones of the Barud area for the tectonics of the North Eastern Desert.

The studied area represents a part of the central Eastern Desert of Egypt; it covers by crystalline basement rocks. It is bounded by latitudes 26° 39` and 26° 43` N and longitudes 33° 36` and 33° 43` E (Figure 1). The area of study is far from the Red Sea about 40 km west of Safaga City. The area can be reached through Qena-Safaga paved road which passes through unpaved wadi Abu Mayah. This wadi has long 30km, and width 50m to 200m, and covered by stream sediments. This wadi represented by three branches with minor drainages. This wadi collected the weathering from G. Um Taghar Al Fuqani (900 a. s. l.), G. Um Tagher Al Tahtany (850m a. s. l.), G. Abu Furad (1032m a. s. l.), so generally, the area is characterized by rugged topography represented by moderate to very high mountains due to the presence of these mountains (Figure 1).

GEOLOGY

The rocks cropping out in the area are represented by metagabbros (oldest), older granitoids (tonalite-granodiorite), and younger granites (youngest).

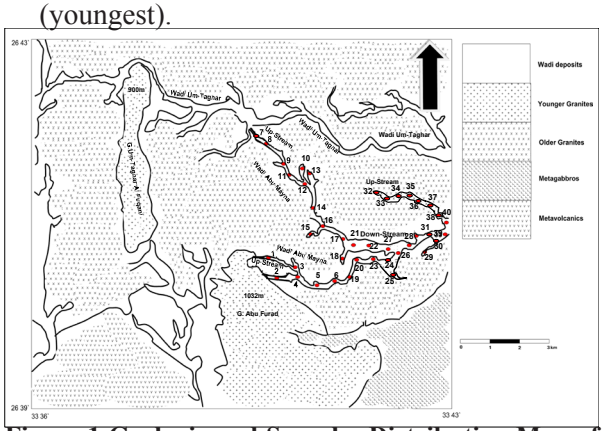

Figure 1 Geologic and Samples Distribution Map of The Area (Modified after Dardier and Al Wakeel, 1998)

The metagabbros are located in the south eastern part of the wadi study and represented by small outcrop (Figure 1). These rocks occur as massive, compact rocks of medium-to-coarse-grained, equigranular with subordinate ophitic and poikilitic textures, greenish grey to whitish green in colour. They are essentially composed of altered plagioclase, amphiboles and very little relics of pyroxene (augite).These rocks are intruded by Abu Furad younger granites from the north. They are frequently injected by quartz veins and veinlets and are intruded by several offshoots of younger granites (Figure 2a).The contact between metagabbros and the younger granites and older granitoids show well defined sharp contact.

The older granitoids are the most common rocks, dominated at all sides of the wadi. The older granitoids are medium to coarse grained, equigranular, hypidiomorphic rocks, calssified as granodiorites and are composed of plagioclase, quartz, orthoclase perthite, biotite and hornblende. They show high weathering such as exfoliation and cavernous features (Figure 2b) and form low hills on vast lands. The wadis traversing these rocks are generally wide, filled with fine to coarse loose sands.

The older granitoids are usually friable and show well developed foliation with gneissose texture, especially along and near contacts. They are grey in colour but become darker near the contacts with metagabbros (Figure 2c). Their colours change to faint pink or whitish pink, especially at the area between G. Um Tagher Al Fuqani and G. Abu Furad, due to the presence of several offshoots of younger granites.

The younger granites are of limited distribution and are represented by G. Um Tagher Al Fuqani and G. Abu Furad (Figure 1). The younger granites of Gabal Um Tagher Al Fuqani and Gabal Abu Furad have the same textural and mineralogical compositions (Figure 2d). They are medium-to-coarse-grained, hypidiomorphic rocks, classified as syenogranites and are composed essentially of perthites, quartz, plagioclase and biotite as well as subordinate amounts of muscovite. G. Um Tagher Al Fuqani is cropping out as elongated belt trending in the N-S direction just south Qena-Safaga high way. The younger granites are distinguished by their red to

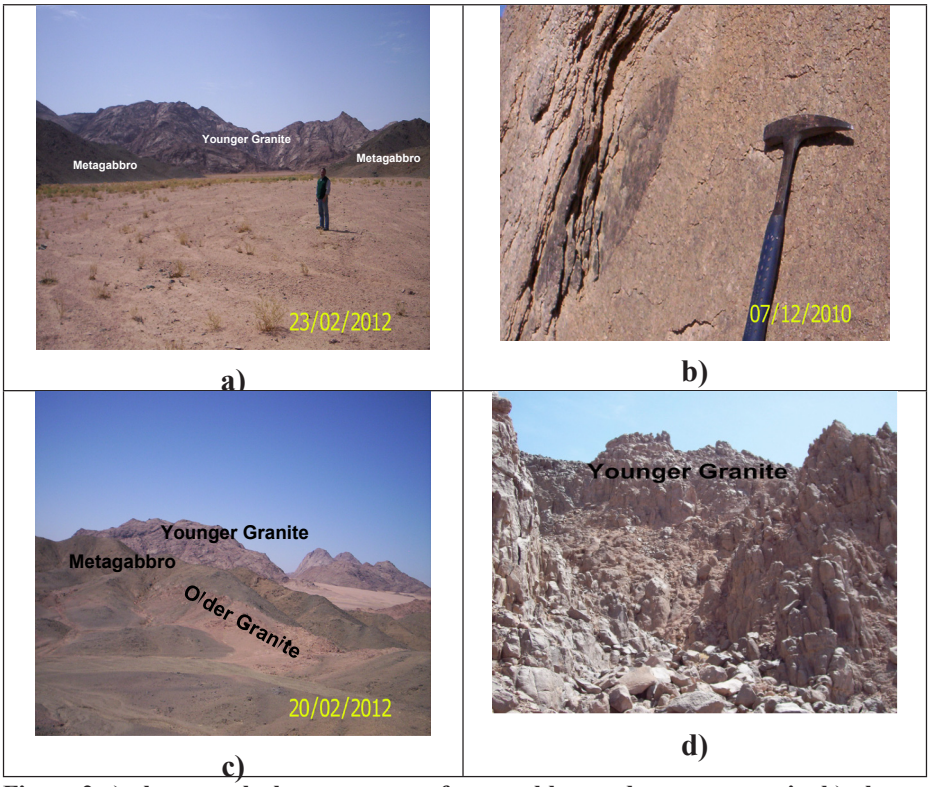

Figure 2 a) photograph show outcrops of metagabbro and younger granite b) photograph show xenolith and X-foliation c) photograph show outcrops of metagabbro and older granite d) photograph show outcrops of younger granite.

pink colours, massive appearance. This granite has xenolith from the older rocks. G. Abu Furad is located southeast of wadi Al Mayah. G. Um Tagher as an oval-shaped belt trending in the N-S direction. They intrude the older rock units with typical intrusive contact and take several xenoliths from older rocks. The size and number of these xenoliths increase near the contacts with the metagabbros. They also send several offshoots into the surrounding rocks.

This granites are characterized by the presence of numerous pegmatitic bodies mainly of zoned, and unzoned types. Dardier and Al Wakeel 1998 said that these Pegmatites are related to the younger granites, but some of them are recorded invading the older granitoids especially on the peripheral zones of the granitic masses, occur as pockets, lenses or small veins, and are limited dimension not exceeding 10 m^2. These pegmatites are abundantly encountered at the northern and eastern parts of G. Abu Furad granitic mass and at different elevations.

The area are dissected by numerous basic and acidic dykes which have mainly NW-SE, NE-SW and nearly E-W directions. They are variable length (1-3 km) and width (1-3m). Faults affecting on the area are limited and either path through the main wadis and the minor wadis, so the drainage patterns are structurally control. These faults are represented by sinistral and dextral strike-slip type.

Materials and Methodology of Study

Forty channel samples were collected from the area around Wadi Abu Mayah from pore holes having about 50cm diameter, and 0.80-1m depth, and some trenches having about 3m length, 1m width, and 1m depth (Figure 3a-d), with intervals ranging from 500-750m (Figure 1). The average weight of each sample is about 10kg. The air-dried original sample was sieved using 2 mm screen. The obtained fraction less than 2mm was quartered using June's splitters of different chutes, down to about 250 gm. Then the obtained representative sample is washed carefully several times to clarify it from silt and clay. Hydrogen peroxide was used to get rid of the organic matters.

A representative sub-sample weighting about 60 gm was taken from each prepared sample by quartering for mineral separation. Separation was conducted using bromoform (Sp.Gr. 2.86g/cm^3) and magnetic fractionation using a Frantz Isodynamic Magnetic Separator (Model L-1). The obtained fractions were carefully studied using the Binocular Stereomicroscope.

In the present study, the collected 40 stream

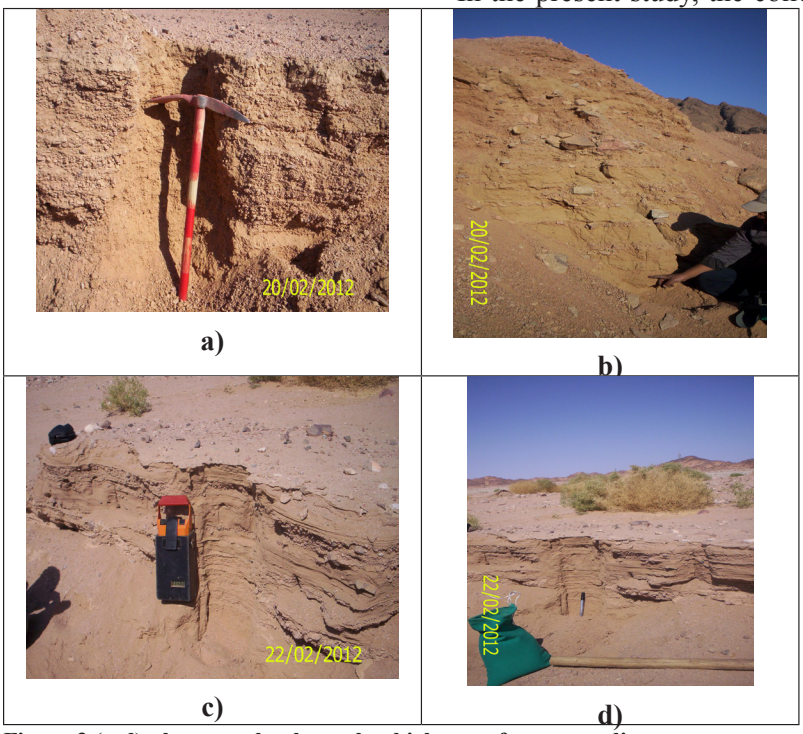

Figure 3 (a-d) photographs show the thickness of stream sediments

sediment samples were analyzed for some trace elements. The elements were determined by XRF techniques on pressed powder pellets. Mineralogical identification of the mineral constituents of the stream sediments was carried out by X-ray diffraction technique. A Phillips X-ray diffractometer (Model PW-1010) with a scintillation counter (Model PW-25623/00) and Ni filter was used. Semiquantitative EDX chemical analyses were carried out using a Phillips XL-30 Environmental Scanning Electron Microscope (ESEM).

The spectrometric study were done in Gamma-Ray Spectrometric laboratory. The cylindrical plastic containers, of volume 212.6 cm^3, 9.5 cm average diameter, and 3 cm length was filled with 300–400gm of the samples, tightly sealed, and left for 30 days to accumulate free radon and attain radioactive equilibrium. The four standards eU, eTh, Ra, and K were measured twice, 1000 seconds for each; the average of gross counts was taken, then divided by their net weight, and introduced to a computer program (Matolin,1990), which runs under Ms-Dos to be used as a matrix of sensitivities represented as the concentrations of eU, eTh, Ra and K. These concentrations are used as a reference for the studied samples. The latter were measured in the same way by means of the computer program which gives out the concentrations of eU and eTh in ppm.

MINERALOGY

Heavy minerals distribution

The average content of the heavy minerals in the studied stream sediments is 5.4 % ranging from 2.94% to 9.4% (Table 1). The content of the heavy minerals in the studied stream sediments have high concentration at upstream and low concentration at downstream. The weight percentage of each concerned mineral relative to the corresponding original sample was calculated, and represented by histogram (Figure 4).

The common heavy minerals in the studied stream sediments are zircon, titanite, monazite, garnet, rutile, thorite, green silicates (amphiboles & pyroxenes) in addition to opaque minerals magnetite, ilmenite (Table 2).

Table 1 The percentages of the heavy minerals in the studied stream sediments of Wadi Abu Mayah

S. No.	Heavy Minerals %	S. No.	Heavy Minerals %
1	9.38	21	3.674
2	9.001	22	4.72
3	8.006	23	4.617
4	8.06	24	4.281
5	7.92	25	4.051
6	7.94	26	4.413
7	7.81	27	3.96
8	7.27	28	3.74
9	6.874	29	4.18
10	6.148	30	4.291
11	6.295	31	3.746
12	6.05	32	3.875
13	6.06	33	3.57
14	6.70	34	3.643
15	5.27	35	3.882
16	5.74	36	3.832
17	5.82	37	4.221
18	5.165	38	3.861
19	5.45	39	3.991
20	5.563	40	2.944
Min.	2.94		
Max.	9.38		
Ave.	5.4		

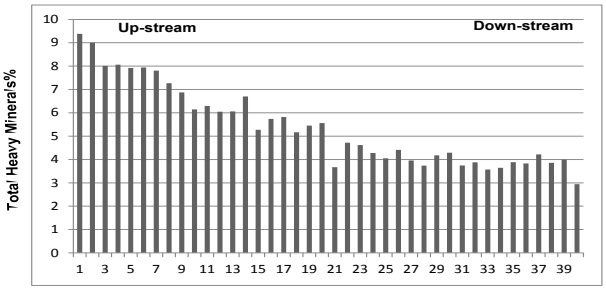

Figure 4 show the distribution histogram for the total heavy minerals

Magnetite (Fe_3O_4)

Magnetite was picked by hand magnet from the studied samples. It is characterized by an opaque and black color, rounded to sub-rounded grains and strongly magnetic, (Figure 5a). The mineral content in the samples range from 0.4% to 2.4 % with an average 1.19 %, and represented by histogram (Figure 5b).

Ilmenite ($[FeTiO_3]$)

It is commonly angular grains with metallic luster, black colors (Figure 5c). Ilmenite is the most abundant Fe-Ti oxide mineral.

The mineral content in the samples range from 0.1% to 1 % with an average 0.4 %, and represented by histogram (Figure 5d).

Garnet [$Fe_3Al_2(SiO_4)$]

Garnet which crystallizes in the isometric system, is mainly formed of angular to sub-rounded

Table 2 The weight percentages of the concerned heavy minerals in the Wadi Abu Mayah stream sediments.

S. No.	Mag.	Ilm.	Gar.	Rut.	Tit.	Zr.	Mz.	Apat.	Tho.	Amph. & Pyr.	Total Heavy
1	2	1.0	0.8	0.3	0.3	0.4	0.09	0.05	0.04	4.4	9.38
2	1.7	0.8	0.3	1.1	0.5	0.9	0.04	0.031	0.03	3.6	9.001
3	1.6	0.5	0.5	0.7	0.2	0.6	0.04	0.026	0.04	3.8	8.006
4	2.4	0.9	0.05	0.1	0.3	0.4	0.05	0.05	0.04	3.8	8.06
5	2.1	0.9	0.5	0.8	0.4	0.6	0.06	0.03	0.03	2.5	7.92
6	1.8	0.9	0.5	0.5	0.3	0.3	0.07	0.05	0.02	3.5	7.94
7	1.7	0.6	0.3	0.5	0.3	0.4	0.05	0.03	0.03	3.9	7.81
8	2.2	0.9	0.04	0.21	0.2	0.3	0.04	0.03	0.03	3.3	7.27
9	1.5	0.7	0.3	0.9	0.3	0.4	0.03	0.024	0.02	2.7	6.874
10	1.6	0.5	0.2	0.2	0.3	0.4	0.01	0.028	0.01	2.9	6.148
11	1.6	0.5	0.3	0.4	0.2	0.5	0.01	0.025	0.03	2.73	6.295
12	1.5	0.7	0.06	0.3	0.03	0.2	0.03	0.04	0.003	3.2	6.05
13	1.6	0.8	0.05	0.2	0.02	0.2	0.04	0.03	0.01	3.1	6.06
14	1.8	0.9	0.04	0.1	0.2	0.1	0.02	0.04	0.02	3.5	6.70
15	1.2	0.5	0.07	0.22	0.02	0.3	0.01	0.03	0.002	3.0	5.27
16	2.1	0.7	0.05	0.1	0.1	0.2	0.05	0.02	0.01	2.4	5.74
17	1.0	0.3	0.4	0.3	0.3	0.4	0.001	0.02	0.001	3.1	5.82
18	1.1	0.2	0.1	0.25	0.2	0.2	0.01	0.005	0.001	3.1	5.165
19	1.6	0.7	0.3	0.6	0.3	0.5	0.08	0.04	0.03	2.9	5.45
20	1.5	0.5	0.2	0.3	0.4	0.3	0.02	0.033	0.01	2.3	5.563
21	0.7	0.1	0.01	0.15	0.01	0.2	0.001	0.004	0	2.5	3.674
22	1.2	0.4	0.2	0.2	0.1	0.4	0.001	0.01	0.01	2.2	4.72
23	1	0.1	0.03	0.4	0.1	0.1	0.01	0.007	0.001	2.9	4.617
24	0.7	0.5	0.05	0.6	0.03	0.1	0.001	0.001	0.00	2.3	4.281
25	0.5	0.1	0.01	0.1	0.2	0.04	0.001	0.001	0.001	3.1	4.051
26	0.9	0.1	0.02	0.18	0.01	0.2	0.001	0.003	0	3.0	4.413
27	0.9	0.1	0.01	0.12	0.01	0.4	0.002	0.02	0.002	2.4	3.96
28	0.8	0.1	0.2	0.10	0.02	0.3	0.004	0.01	0.001	2.2	3.74
29	1.1	0.3	0.03	0.2	0.03	0.2	0.01	0.01	0.001	2.3	4.18
30	0.8	0.1	0.02	0.2	0.1	0.06	0.01	0.02	0.001	3.0	4.291
31	0.8	0.1	0.01	0.2	0.02	0.1	0.01	0.006	0.00	2.5	3.746
32	0.7	0.2	0.02	0.21	0.03	0.1	0.01	0.005	0	2.6	3.875
33	0.5	0.1	0.04	0.2	0.2	0.02	0.005	0.004	0.001	2.5	3.57
34	1	0.2	0.04	0.18	0.1	0.01	0.007	0.003	0	2.1	3.643
35	0.9	0.3	0.01	0.3	0.02	0.05	0.001	0.002	0.00	2.3	3.882
36	1.0	0.2	0.02	0.4	0.04	0.07	0.001	0.002	0.00	2.1	3.832
37	0.9	0.3	0.04	0.5	0.02	0.06	0.001	0.001	0.00	2.4	4.221
38	0.7	0.3	0.03	0.5	0.03	0.1	0.001	0.001	0.00	2.2	3.861
39	0.5	0.4	0.05	0.6	0.04	0.1	0.001	0.001	0.00	2.3	3.991
40	0.4	0.1	0.01	0.1	0.1	0.03	0.001	0.001	0.001	2.2	2.944
Min.	0.4	0.1	0.01	0.1	0.01	0.01	0.001	0.001	0.001	2.1	2.94
Max.	2.4	1	0.8	1.1	0.5	0.9	0.09	0.05	0.04	4.4	9.38
Aver.	1.195	0.44	0.15	0.34	0.152	0.256	0.021	0.011	0.019	2.821	5.4

Mag.=magnetite, Ilm.=ilmenite, Gar.=garnet, Rut.=rutile, Tit.=titanite, Zr.=zircon, Mz.=monazite, Thrt.=thorite, Amph.&Pyr.=amphibles and pyrxenes.

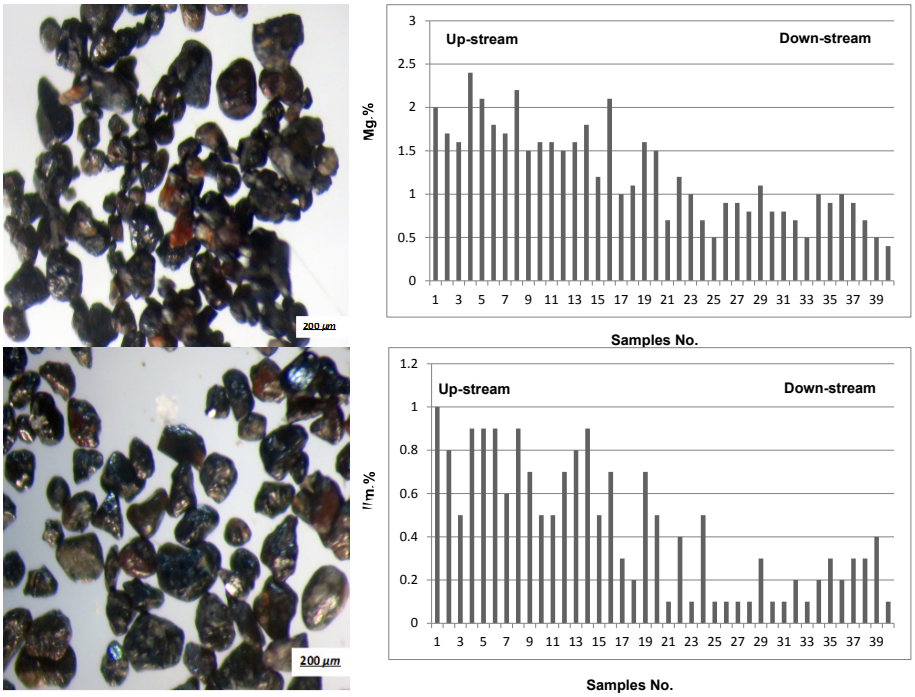

Figure 5 Shows a) Photomicrograph for the magnetite b) histogram distribution for magnetite c) photo-micrograph for ilmenite d) histogram distribution for ilmenite

particles. Its grain size is relatively coarser than the other economic minerals of the study samples. Garnet is the pale pink color (Figure 6a), and has moderate magnetic susceptibility which varies slightly according to variation in chemical composition (Milner, 1962). The mineral content in the samples range from 0.01% to 0.8 % with an average 0.15 %, and represented by histogram (Figure 6a). It detected using EDX technique (Figure 6b)

Rutile [TiO_2]: It is the preferred mineral for the production of titanium dioxide. Rutile mineral grains are commonly prismatic, elongated, tabular and massive granular in shape. The common colors of rutile are reddish brown grading into the red (Figure 6c) and black with adamantine luster. The mineral content in the samples ranges from 0.1% to 1.1% with an average 0.34%, and represented by histogram (Figure 6d).

Sphene (Titanite) [$CaTiSiO_5$]

Sphene is widespread in acidic and intermediate igneous rocks, and in several metamorphic rocks as accessory mineral. Titanite mineral grains are subhedral to anhedral of adamantine luster. It exhibits transparent to translucent yellow to yellowish brown colors (Figure 6e). The mineral content in the samples ranges from 0.01% to 0.5 % with an average 0.15 %, and represented by histogram (Figure 6e). It detected using EDX technique (Figure 6f).

Zircon [$ZrSiO_4$]

It occurs as euhedral grains honey yellow, red, black and grey colors of adamantine luster, zircon well preserved as euhedral crystals with bipyramidal termination while few zircon grains are prismatic crystals forms (Figure 7 a & b). The mineral content in the samples ranges from 0.01% to 0.5 % with an average 0.15 %, and represented by histogram (Figure 7c). It detected using EDX technique (Figure 7d).

Monazite [$CePO_4$]: is one of the most important nuclear minerals, being a major host for REEs and actinides Th and U (Hinton and Pater-

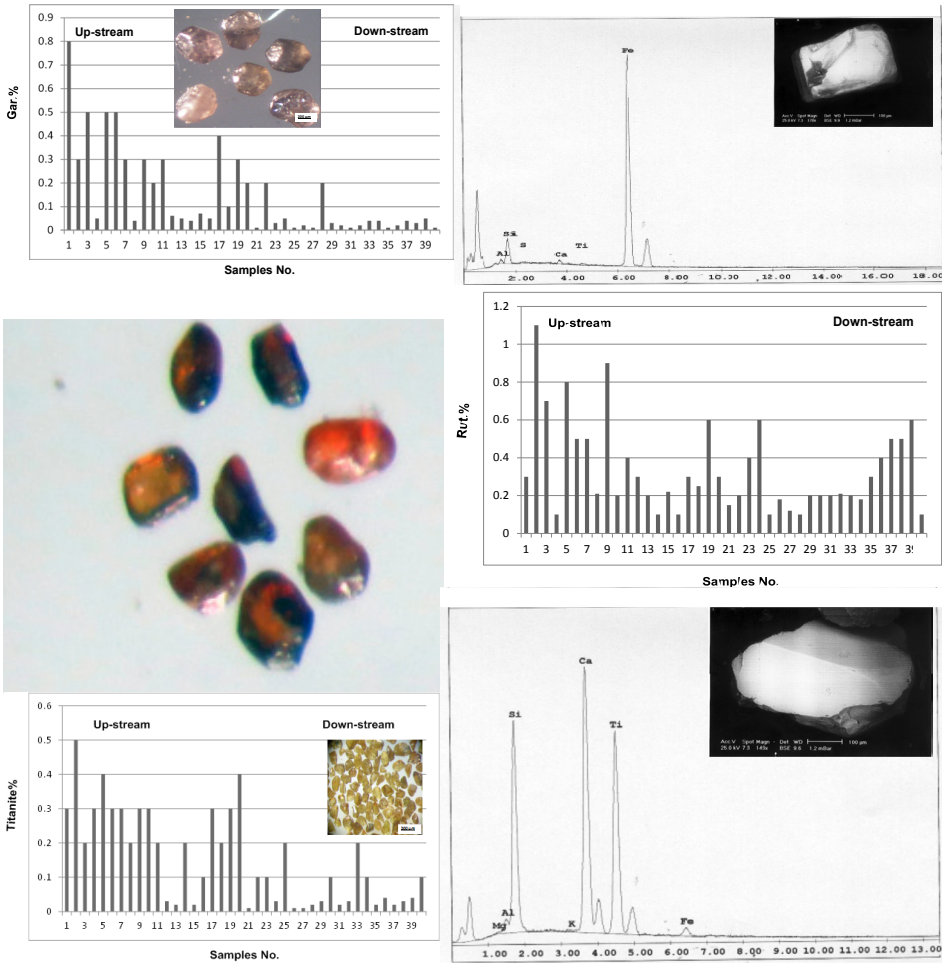

Figure 6 Show a) photo-micrograph for garnet within histogram distribution for garnet b) ESEM garnet analysis c) photo-micrograph for rutile d) histogram distribution for rutile e) photo-micrograph for titanite within histogram distribution for titanite f) ESEM titanite analysis.

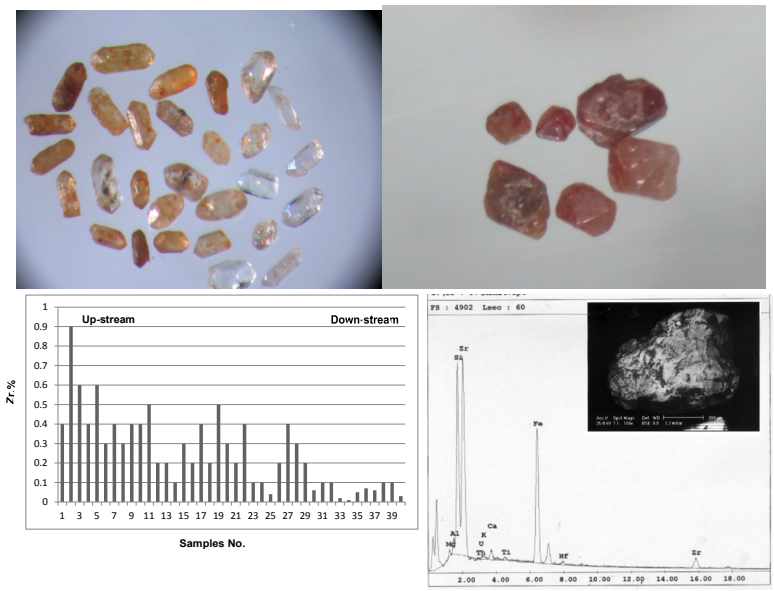

Figure 7: Show a, & b) photo-micrographs for colourless, yellow, and brown zircon) c) histogram distribution for zircon d) ESEM zircon analyses.

son 1994, Bea et al. 1994, Bea 1996). Monazite in the studied samples is rare. It forms rounded to well-rounded pale yellow, honey yellow, greenish yellow and reddish yellow grains (Fig. 8a). The mineral content in the samples range from 0.001% to 0.09 % with an average 0.021%, and represented by histogram (Figure 8b). Most of these grains are characterized by pitted surfaces.

Apatite: This minerals is rare and characterized by colorless, oval shape and most of these grains are characterized by pitted surfaces (Fig. 8c). It contains rare earth elements. The mineral content in the samples range from 0.001% to 0.04 % with an average 0.01%, and represented by histogram (Fig. 8d)..

Thorite [$ThSiO_4$]: It occurs widely in the form of accessory minerals, which belong to the most important basic commercial minerals of thorium. It occurs as brownish black to black opaque grains of greasy luster (Figure 9a). Most of thorite mineral grains are subhedral to anhedral corroded and cracked. They are strongly metamictized, as determined by X-ray diffraction. In nature, thorite, generally, occurs in metamict state, amorphous to X-ray and electron diffraction, even though, they may have crystal

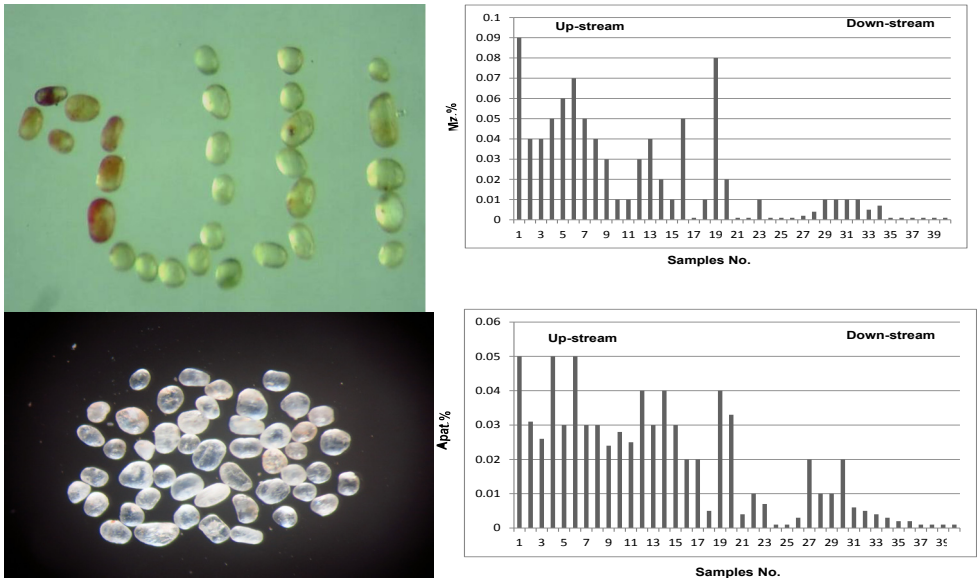

Figure 8 Show a) photo-micrograph for Monazite b) histogram distribution for monazite c) photo-micrograph for Apatite d) histogram distribution for Apatite

faces (Palache et al 1944, Pabst 1952, Ewing and Haaker 1980). Thorite was annealed at 1100˚C for approximately four hours preceding identification by XRD. The obtained data (Table 3) reveal the presence of thorite peaks (ASTM card 11-419) in addition to hematite peaks (ASTM card 13-534). The presence of hematite may be in the form of thin films coating thorite grains or as individual hematite grains. The mineral content in the samples range from 0.001% to 0.03% with an average 0.001%, and represented by histogram (Figure 9a). The ESEM analysis shows that thorite consists mainly of ThO_2 and SiO_2. Minor and trace elements include Y, U, Ca, Fe and REE (Figure 9b).

Amphiboles and Pyroxene These minerals may have originated from metamorphic and igneous rocks. These minerals are characterized by coarse size detrital particles, black, green colour, coarse grains, and present in 0.2 and 0.5 ampere magnetic. The mineral content in the samples range from 2.1% to4.4 % with an average of 2.81%, and represented by histogram (Fig. 9c **).**

Table 4: X-ray diffraction data of the annealed thorite from the studied stream sediments.

Analyzed Sample		Thorite ASTM card (11-419)	
dA	I/Io	dA	I/Io
4.73	72	4.72	85
3.54	90	3.55	100
2.87	35	2.842	45
2.66	51	2.676	75
2.53	27	2.516	30
2.20	30	2.222	30
2.03	15	2.019	20
1.87	18	1.885	30
1.80	30	1.834	65
1.78	18	1.782	20

Geochemical Study

The results of XRF analysis of the trace elements for the stream sediments samples are tabulated in (Table 5). The Table shows that, the stream sediments samples are rich in Zr, Nb, Rb, and Y. It is clear that, the stream sediments are highly affected by the surrounding rocks. The distribution of these elements were explained by histograms and lateral diagrams (Figures 10a-d, and 11a-d). From these distributions the elements concentrated at up-stream near the G. Um Taghar Al Fuqani and G. Abu Furad and the low concentration of minerals at down-stream.

Radiometric Study

A total of 40 stream sediments samples had been collected from the studied area throughout systematic sampling to determine variations in eU, eTh, and K%. The obtained results from the radiometric measurements of the studied stream sediments are listed in Table 6, and calculate the ratios of eTh/eU. Draw the histograms distribution for these elements and ratios (Figure 12 a-d and 13a-d).

The examined stream sediments of Wadi Abu Mayah are characterized by radiometrically moderately to highly concentrations of uranium and thorium. The radiometrically elemental concentration of eU range between 12 and 40ppm with an average 21.36ppm, while eTh is between 20 and 86ppm for with an average 38.2ppm. The average content of K% 1.5%, ranging between 0.8 and 2.4.

Ivanovich (1994) concluded that a relatively constant Th/U mass ratio of around 3.5 is found in most natural systems. The average of the corresponding value (eTh/eU ratio) for the sediments of Wadi Abu Mayah is 1.8 varying between 1.2 and 2.4 which indicate that there is a significant fractionation during weathering of these sediments causing the depletion of U.

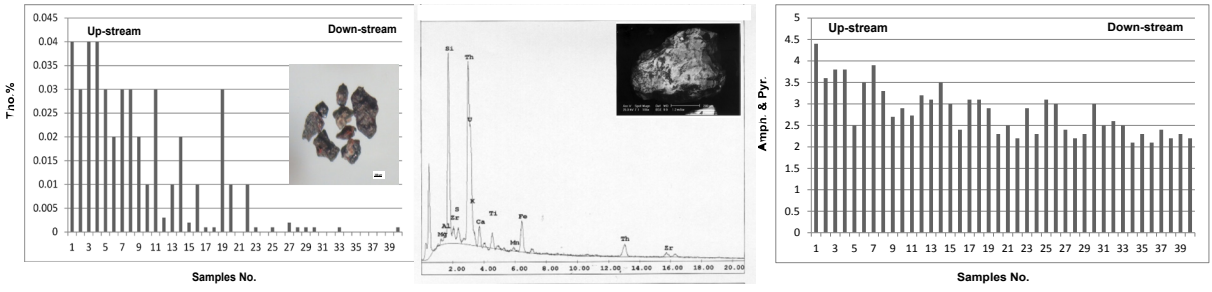

Figure 9 Show a) photo-micrograph for thorite within histogram distribution for thorite b) ESEM thorite analyses c) histogram distribution for amphiboles and pyroxenes.

Table 5 XRF Analysis of stream sediments samples at Wadi Abu Mayah (ppm).

S. No.	Cr	Ni	Nb	Zr	Rb	Y	Ba	Pb	Sr	Ga
1	5	64	95	380	202	75	140	65	60	25
2	4	51	85	370	201	67	138	71	51	23
3	3	50	81	340	198	58	136	68	57	21
4	2.7	45	83	325	190	55	135	64	49	24
5	1.5	42	84	300	186	52	131	58	42	20
6	3	38	78	295	184	41	128	59	41	26
7	4	52	75	291	182	40	126	57	40	20
8	2.4	62	71	285	179	36	100	46	37	23
9	3.1	40	73	250	174	34	92	31	38	24
10	3	35	72	291	170	31	85	30	27	27
11	3	32	75	275	168	35	64	32	25	25
12	2	28	45	276	95	34	52	24	25	29
13	2	42	53	245	84	31	42	23	24	25
14	2.1	40	38	234	78	30	38	27	28	26
15	2.4	32	42	237	81	28	30	21	26	28
16	2.0	28	34	220	75	27	34	20	22	24
17	2	25	33	195	72	26	28	31	20	20
18	3	22	32	175	68	28	29	30	28	21
19	2	20	35	181	62	24	34	23	24	23
20	3	21	33	172	63	28	31	24	21	25
21	4	20	31	165	60	25	30	21	21	29
22	5	24	38	189	90	43	37	47	34	27
23	3	21	45	215	98	45	48	52	33	34
24	5	26	57	224	150	58	53	61	38	38
25	4	23	68	245	155	64	55	71	34	34
26	4	25	75	258	168	67	57	70	39	39
27	3	27	72	267	167	60	69	75	45	48
28	4	22	84	281	177	65	73	71	54	45
29	5	21	81	280	180	72	80	65	60	46
30	3	20	61	168	72	51	51	50	41	29
31	2	18	54	152	65	42	43	41	40	30
32	1	17	21	145	61	34	40	32	38	27
33	2	18	24	150	57	33	40	33	34	22
34	2	17	25	140	54	31	30	30	32	24
35	1	19	21	135	50	28	34	41	31	26
36	1	16	20	130	41	21	32	24	30	28
37	3	15	35	145	45	20	30	29	36	30
38	3	18	34	150	38	24	24	27	34	31
39	4	17	48	132	34	23	20	28	35	32
40	5	16	48	125	33	20	21	31	30	33

eU versus eTh variation diagram

The relation between U and Th may indicate the enrichment or depletion of U because Th is chemically stable. The eU against eTh variation diagram for the studied samples is shown in Figure 14a, which indicates strong positive relationships between the two elements. This result explains the low alteration processes affecting on these samples, and also indicates that magmatic processes played an important role in the uranium enrichment of these granites which represent the source of these sediments.

eU versus Zr variation diagram

The eU versus Zr variation diagram shows strong positive correlation in the studied samples (Figure 14b). The uranium and zirconium enrichment in the studied samples, supports the concept that U was trapped in the accessory minerals as zircon and the uranium is magmatically.

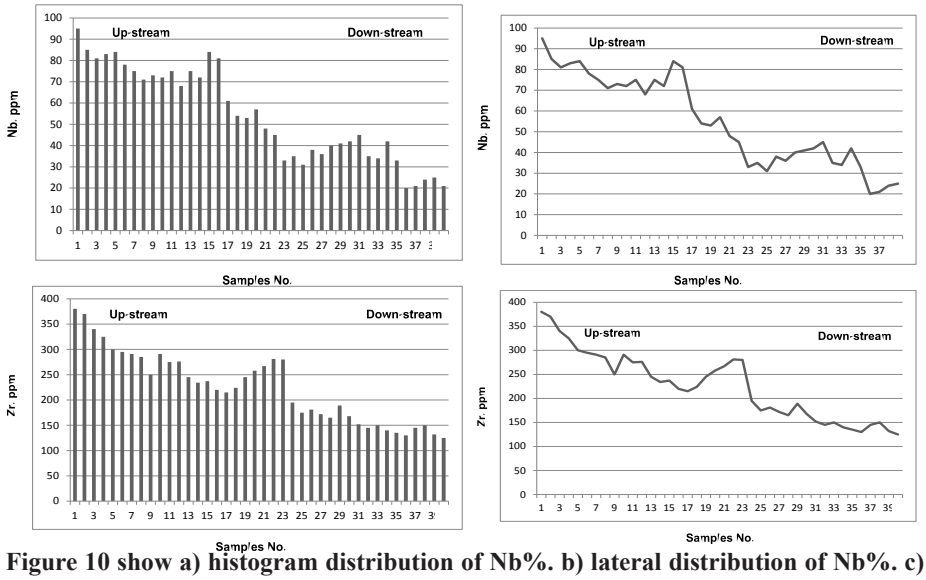

Figure 10 show a) histogram distribution of Nb%. b) lateral distribution of Nb%. c) histogram distribution of Zr%. b) lateral distribution of Zr%.

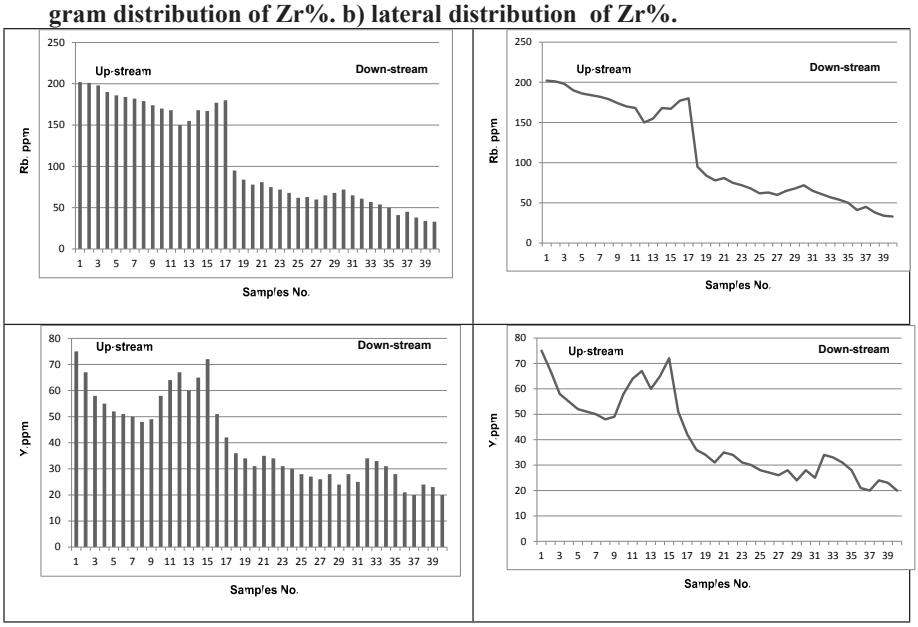

Figure 11 show a) histogram distribution of Rb% b) lateral distribution of Rb% c) histogram distribution of Y%. b) lateral distribution of Y%.

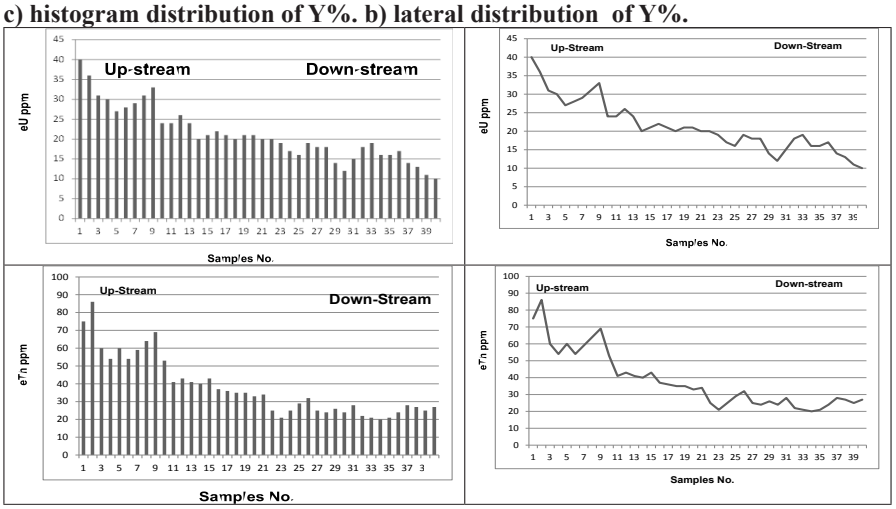

Figure 12: show (a) the histogram distribution of equivalent uranium (b) lateral distribution of equivalent uranium (c) the histogram distribution of equivalent thorium (d) lateral distribution of equivalent thorium.

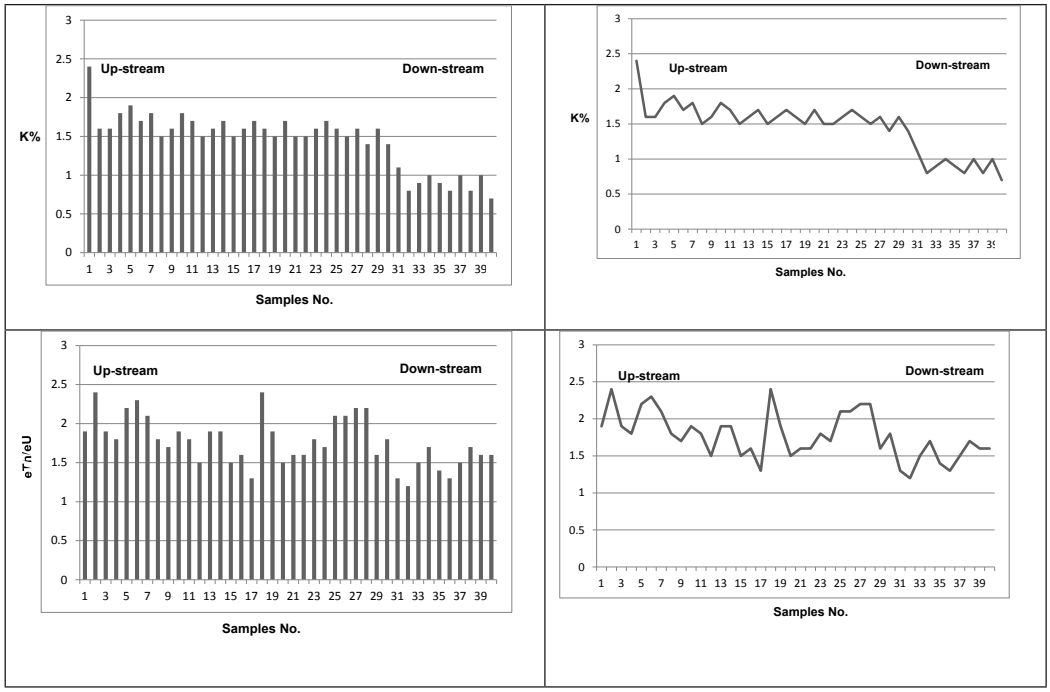

Figure 13 show a) histogram distribution of K%. b) lateral distribution of K%. c) histogram distribution of eTh/eU. d) lateral distribution of eTh/eU.

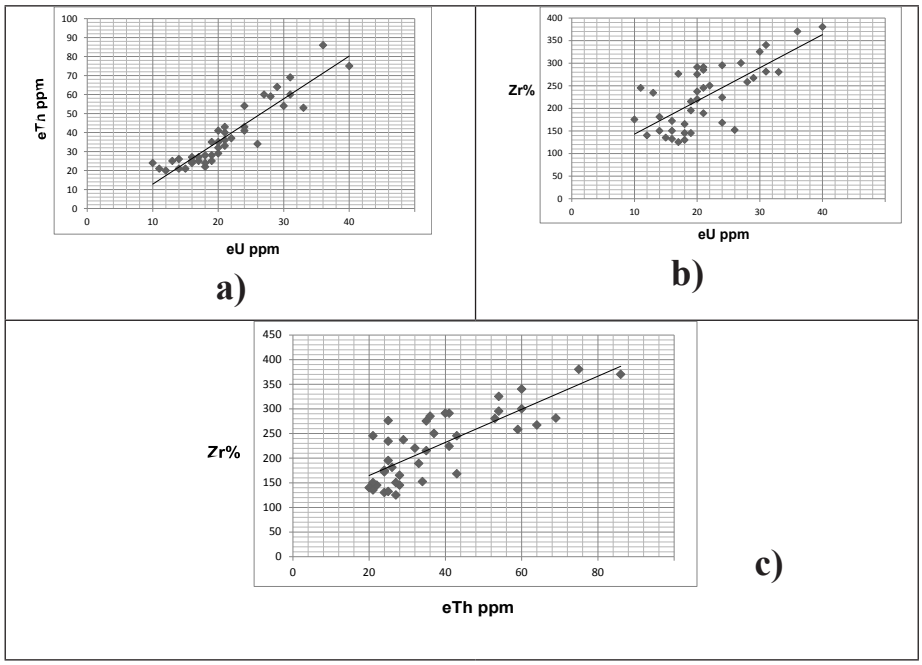

Figure 14 Show a) direct relationship between equivalent uranium and equivalent thorium. (b) direct relationship between eU and concentration of Zr minerals. C) direct relationship between eTh and concentration of Zr minerals.

Conclusion

The study concerned with the study of economic minerals in the stream sediments of wadi Abu Mayah which has long 30km and width reach to 50m**.** The area covered by igneous and metamorphic rocks represented by Metagabbro, Older Granite, and Younger Granite.

The average content of total heavy minerals is 5.4% and the heavy content ranging from 2.9% and 9.4%. Opaque minerals represented by Magnetite, Ilmenite constituents have an average 1.2 %, and 0.4 % respectively. Abrasive minerals as Garnet constituents has an average 0.15%, and panting minerals as Rutile and Ti-

Table 3 The Radiomtric Measurements of the studied stream sediments samples

S. No.	eU ppm	eTh ppm	K (%)	eTh/eU
1	40	75	2.4	1.9
2	36	86	1.6	2.4
3	31	60	1.6	1.9
4	30	54	1.8	1.8
5	27	60	1.9	2.2
6	24	54	1.7	2.3
7	20	41	1.2	2.1
8	21	36	1.5	1.8
9	22	37	1.3	1.7
10	21	40	1.8	1.9
11	20	35	1.7	1.8
12	17	25	1.1	1.5
13	11	21	1.2	1.9
14	13	25	1.7	1.9
15	20	29	1.3	1.5
16	20	32	1.1	1.6
17	19	25	1.9	1.3
18	10	24	1.6	2.4
19	14	26	1.5	1.9
20	16	24	1.7	1.5
21	18	28	1.3	1.6
22	21	33	1.8	1.6
23	19	35	1.9	1.8
24	24	41	1.7	1.7
25	21	43	2.0	2.1
26	28	59	1.9	2.1
27	29	64	1.8	2.2
28	31	69	1.4	2.2
29	33	53	1.6	1.6
30	24	43	1.4	1.8
31	26	34	1.1	1.3
32	18	22	0.8	1.2
33	14	21	0.9	1.5
34	12	20	1.0	1.7
35	15	21	1.1	1.4
36	18	24	1.3	1.3
37	19	28	1.2	1.5
38	16	27	1.1	1.7
39	16	25	1.0	1.6
40	17	27	1.2	1.6
Min.	12	20	0.8	1.2
Max.	40	86	2.4	2.4
Aver.	21.3	38.2	1.5	1.8

tanite constituents have an average 0.34%, and 0.15% respectively. Radioactive minerals as Zircon, Monazite, Apatite and Thorite constituents have an average 0.26%, 0.02%, 0.01, and 0.02 % respectively. Amphiboles and Pyroxene constituents range from 2.1% to 4.4% with an average 2.8 %. The eU contents range between 12 and 40ppm with an average 21.3ppm, while eTh is between 20 and 86ppm for with an average 38.2ppm. The average Ra average content for these sediments is 2.9ppm, and the average content of K% 1.5%.

The transportation agent is rare and consider seasonal so the sediment restricted near the source rock and transported short distance.

REFERENCES

Abdel-Rahman, A. M., 1990. Petrogenesis of early-orogenic diorites, tonalites and post-orogenic trondhjemites in the Nubian shield. J. Petrol. 31, 1285–1312.

Abdel-Rahman Fowler, Khaled G. Ali, Sayed M. Omar, Hassan A. Eliwa, 2006. The significance of gneissic rocks and synmagmatic extensional ductile shear zones of the Barud area for the tectonics of the North Eastern Desert, Egypt Journal of African Earth Sciences 46 201–220

Akaad, M.K., El-Gaby, S., Habib, M.E., 1973. The Barud Gneisses and the origin of Grey Granite. Bull. Fac. Sci. Assiut Univ. 2, 55–69.

Bea, F., 1996. Residence of REE, Y, Th and U in granites and crustal protolith; implications for the chemistry of crustal melt. J. Petrol., Vol. 37, P. 521:552.

Bea, F., Pereira, M. D., Corretage, L. G. and Fershtater, G. B., 1994. Differentiation of strongly peraluminous, perphosphorous granites: the Pedrobenards pluton, Central Spain. Geochemica et Cosmochemica Acta, Vol. 58, P. 2609:2627.

Dardier, A. M., and Al Wakeel, M. I 1998. Geology, Petrology and Radioactivity of Gabal Um Tagher-Gabal Abu Furad Area, Central Eastern Desert, Egypt. Egyptian Journal of Egypt, Vol. 42/1**.**

El Ramly, M. F. and Akaad, M. K., 1960. The basement complex in the Central Eastern Desert of Egypt, between latitudes 24 30 and 25 40N. Geol. Surv. Egypt. Cairo, Vol. 8, P. 35p.

Ewing, R. C. and Haaker, R. F., 1980. The metamict state: Implications for radiation damage in crystalline waste forms. Nuclear and Chemical Waste Management, I, P. 51:57.

Greenberg, J. K., 1981. Characteristics and origin of Egyptian Younger Granites: Summary. Geol. Soc. Amer. Bull, pt. 1, v. 92, 224-232.

Hinton, R. W. and Paterson, B. A., 1994. Crystallization history of granitic magma: evidences from trace elements zoning. Mineral. Mag., Vol. 58A, P. 416:417.

Ivanovich, M., 1994. Uranium series disequilibrium: concept and applications. Radiochem. Acta, Vol. 64, P. 81:94.

Matolin, M., 1990. A report to the Government of the Arab Republic of Egypt "Construction and use of spectrometric calibration pads", Egypt/4/030-03, Laboratory Gamma Ray spectrometry

Milner, H. B., 1962. Sedimentary petrography. V, II, George Allen & Unwin, Ltd., London. pp. 15-205.

Pabst, A., 1952. The metamict state. Am. Mineral. Vol. 37, P. 137:157.

Palache, C., Berman, H. and Frondel, C., 1944. Dana's system of mineralogy. Vol. 1,(7th edition). Wiley, New York.